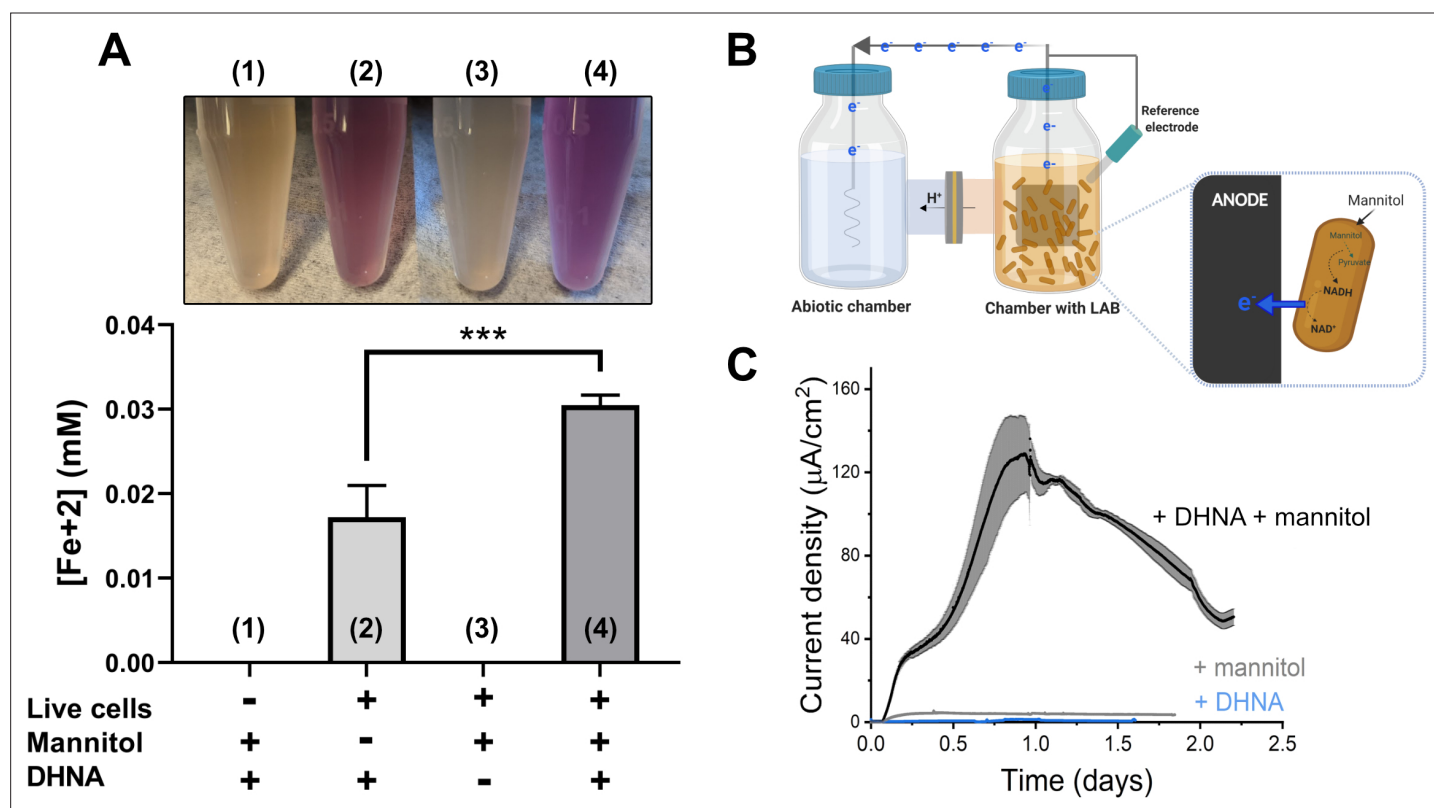


---

## Figures and figure supplements

Extracellular electron transfer increases fermentation in lactic acid bacteria via a hybrid metabolism

**Sara Tejedor-Sanz *et al***



**Figure 1.** *L. plantarum* can reduce both Fe<sup>3+</sup> and an anode through EET. **(A)** Reduction of Fe<sup>3+</sup> (ferrihydrite) to Fe<sup>2+</sup> by *L. plantarum* NCIMB8826 after growth in mMRS. The assays were performed in PBS supplemented with 20 µg/mL DHNA and/or 55 mM mannitol. Fe<sup>2+</sup> was detected colorimetrically using 2 mM ferrozine. For *L. plantarum* inactivation, cells were incubated at 85°C in PBS for 30 min prior to the assay. Significant differences were determined by one-way ANOVA with Tukey's post-hoc test (n = 3), \*\*\* p ≤ 0.001. **(B)** Two-chambered electrochemical cell setup for measuring current generated by *L. plantarum*. **(C)** Current density production over time by *L. plantarum* in CDM supplemented with 20 µg/mL DHNA and/or 110 mM mannitol. The anode was polarized at +0.2V<sub>Ag/AgCl</sub>. The avg ± stdev of three biological replicates is shown. See also **Figure 1—figure supplement 1** and **Figure 1—figure supplement 2** and related data in **Figure 1—source data 1**.

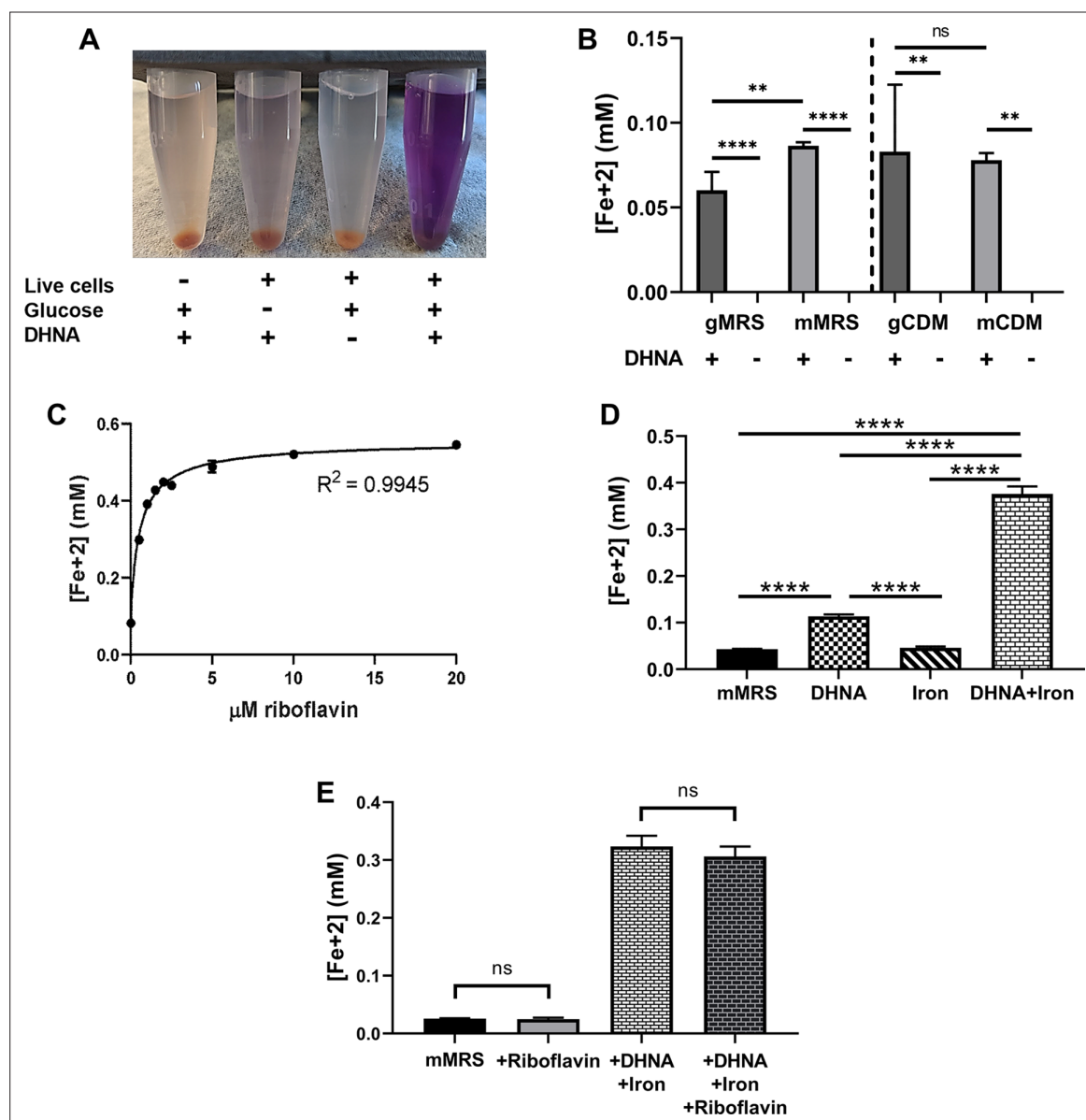


**Figure 1—figure supplement 1.** Iron reduction by *L. plantarum* is dependent upon DHNA, carbon source, and riboflavin. **(A)** Reduction of  $\text{Fe}^{3+}$  (ferrihydrite) to  $\text{Fe}^{2+}$  by *L. plantarum* NCIMB8826 after growth in MRS with glucose (gMRS). The assays were performed in PBS supplemented with 20  $\mu\text{g}/\text{mL}$  DHNA and/or 55 mM glucose. For *L. plantarum* inactivation, cells were incubated at 85°C in PBS for 30 min prior to the assay. **(B)** Reduction of ferrihydrite by *L. plantarum* after growth in MRS with glucose (gMRS) or mannitol (mMRS) or CDM with glucose (gCDM) or mannitol (mCDM). The ferrihydrite reduction assays were performed in PBS supplemented with 20  $\mu\text{g}/\text{mL}$  DHNA and the corresponding carbon source (55 mM glucose or mannitol). **(C)** Reduction of ferrihydrite by *L. plantarum* in the presence of 20  $\mu\text{g}/\text{mL}$  DHNA, 55 mM mannitol, and increasing concentrations of riboflavin. **(D and E)** Reduction of ferrihydrite by *L. plantarum* after growth to mid-exponential phase in mMRS with or without the supplementation of 20  $\mu\text{g}/\text{mL}$  DHNA, iron (1.25 mM ferric ammonium citrate), and/or 2.5  $\mu\text{M}$  riboflavin. Significant differences in iron reduction were determined by one-way ANOVA with Tukey's post-hoc test ( $n = 3$ ), \*\*  $p \leq 0.01$ ; \*\*\*\*  $p \leq 0.0001$ . The avg  $\pm$  stdev of three biological replicates is shown. See related data in **Figure 1—figure supplement 1—source data 1**.

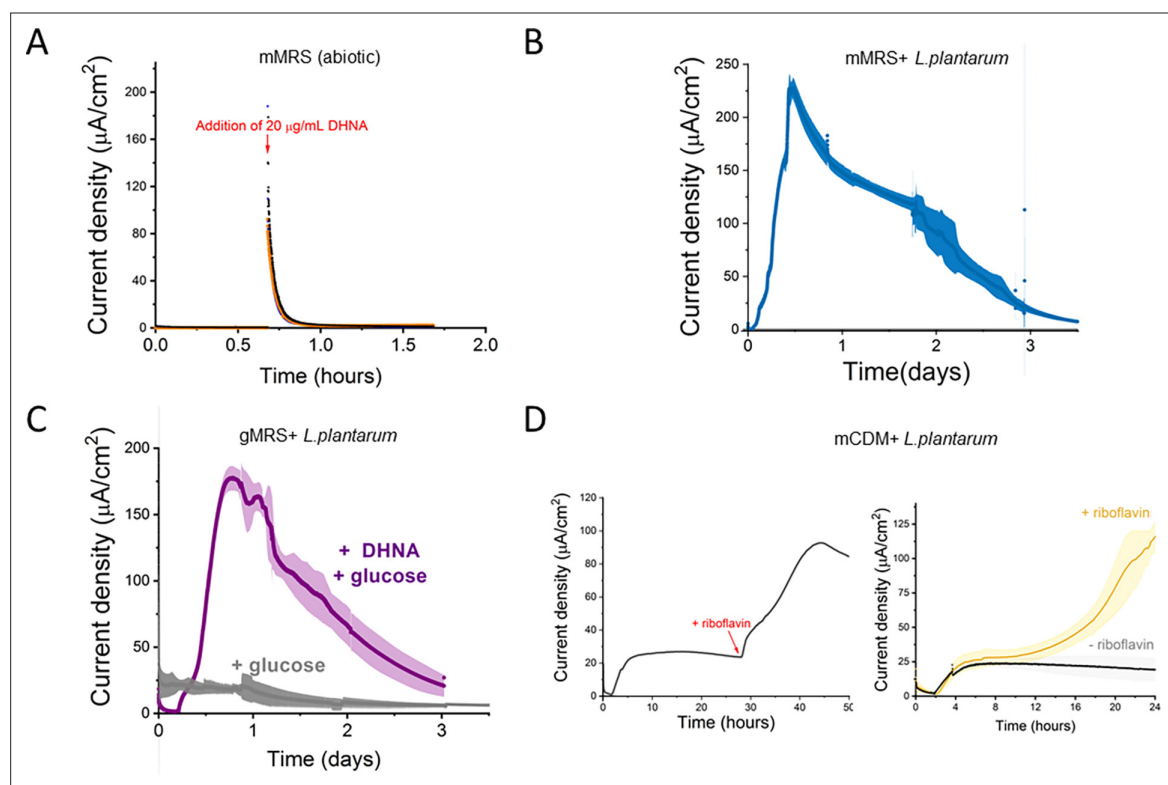


**Figure 1—figure supplement 2.** Current production by *L. plantarum* is a biotic process dependent on DHNA, carbon source, and riboflavin. (A) Abiotic current density response in bioelectrochemical reactors over time in mannitol-containing MRS (mMRS) upon DHNA (20  $\mu\text{g}/\text{mL}$ ) addition. Current density produced by *L. plantarum* in (B) mMRS with 20  $\mu\text{g}/\text{mL}$  DHNA or (C) gMRS with 20  $\mu\text{g}/\text{mL}$  DHNA. (D) Effect of riboflavin addition on current density production by *L. plantarum* in mannitol-containing CDM (mCDM) with 20  $\mu\text{g}/\text{mL}$  DHNA. The avg $\pm$  stdev of three biological replicates is shown. See related data in **Figure 1—figure supplement 2—source data 1**.



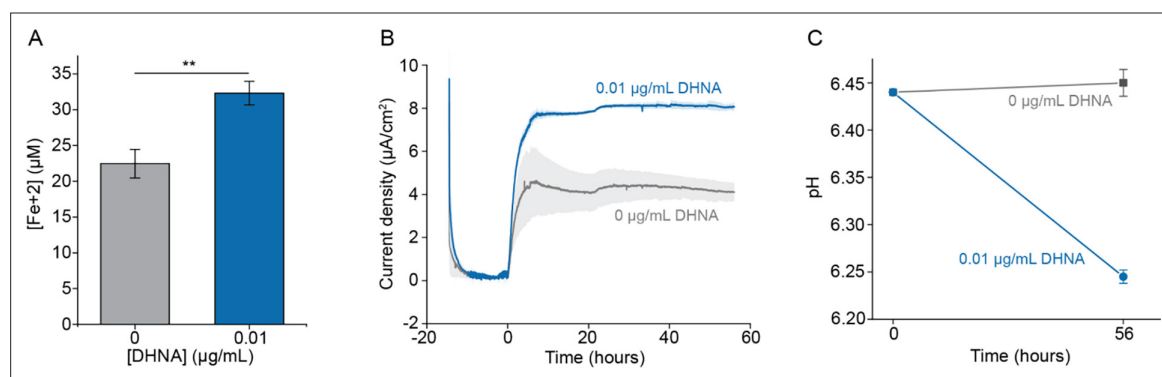


**Figure 1—figure supplement 3.** A sub-physiological concentration of DHNA stimulates EET in *L. plantarum*. Reduction of  $\text{Fe}^{3+}$  (iron III oxide nanoparticle, primarily  $\gamma\text{-Fe}_2\text{O}_3$ ) to  $\text{Fe}^{2+}$  (A) and current production (B) by *L. plantarum* when 0.01  $\mu\text{g/mL}$  DHNA was supplied. (C) pH measurements at 0 and 56 hr for the experiment shown in (B). The avg  $\pm$  stdev is shown. Three replicates for (A) and two replicates for (B) and (C). Significant differences were determined by two-tailed t-test,  $**p \leq 0.01$ . See related data in **Figure 1—figure supplement 3—source data 1**.

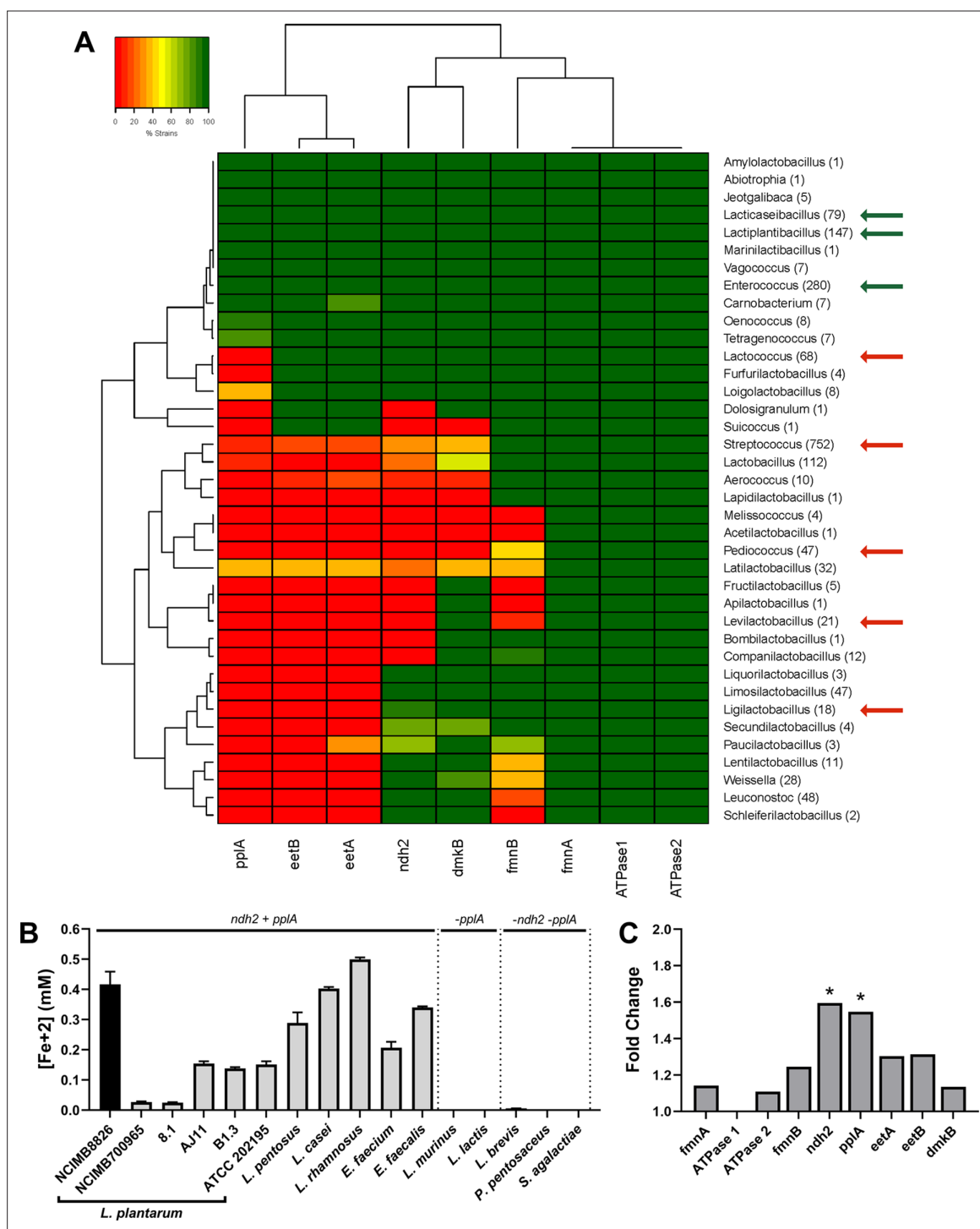


**Figure 2.** The FLEET genes *ndh2* and *pplA* are associated with iron reduction by LAB. **(A)** Heatmap showing the genera in the Lactobacillales order containing FLEET genes. Homology searches were conducted using tBLASTx for 1788 complete LAB genomes in NCBI (downloaded 02/25/2021) against the *L. plantarum* NCIMB8826 FLEET locus. A match was considered positive with a Bit-score >50 and an E-value of  $<10^{-3}$ . Arrows designate genera tested for iron reduction activity; green = EET-active with  $\text{Fe}^{3+}$ , red = EET-inactive with  $\text{Fe}^{3+}$ . **(B)** Reduction of ferrihydrite in PBS with 20  $\mu\text{g}/\text{mL}$  DHNA and 55 mM mannitol after growth in mMRS supplemented with 20  $\mu\text{g}/\text{mL}$  DHNA and 1.25 mM ferric ammonium citrate. The avg  $\pm$  stdev of three biological replicates per strain is shown. **(C)** Relative expression of NCIMB8826 FLEET locus genes in mMRS with 20  $\mu\text{g}/\text{mL}$  DHNA and 1.25 mM ferric ammonium citrate compared to growth in mMRS. Significant differences in expression were determined by the Wald test ( $n = 3$ ) with a  $\text{Log}_2$  (fold change) > 0.5 and an FDR-adjusted p-value of <0.05. See also **Figure 2—figure supplement 1** and **Figure 2—figure supplement 2** and related data in **Figure 2—source data 1**.

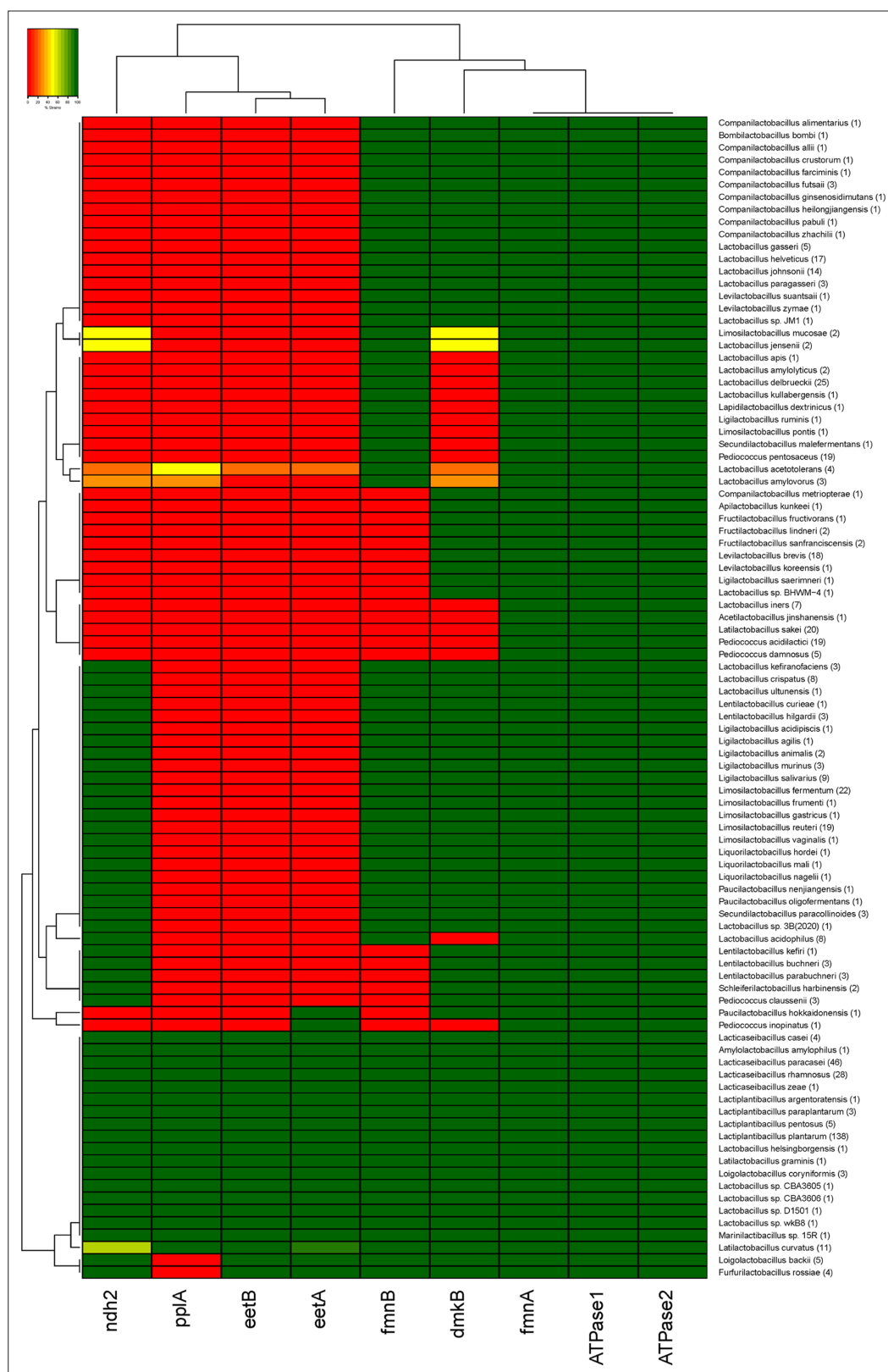


**Figure 2—figure supplement 1.** Conservation of FLEET locus genes among lactobacilli. Heatmap showing the bacteria in the *Lactobacillus*-genus complex containing genes in the FLEET locus. Homology searches were conducted using tBLASTx for 1788 complete LAB genomes in NCBI (downloaded 02/25/2021) against the *L. plantarum* NCIMB8826 FLEET locus. A match was considered positive with a Bit-score >50 and an E-value of <10<sup>-3</sup>. See related data in **Figure 2—figure supplement 1—source data 1**.

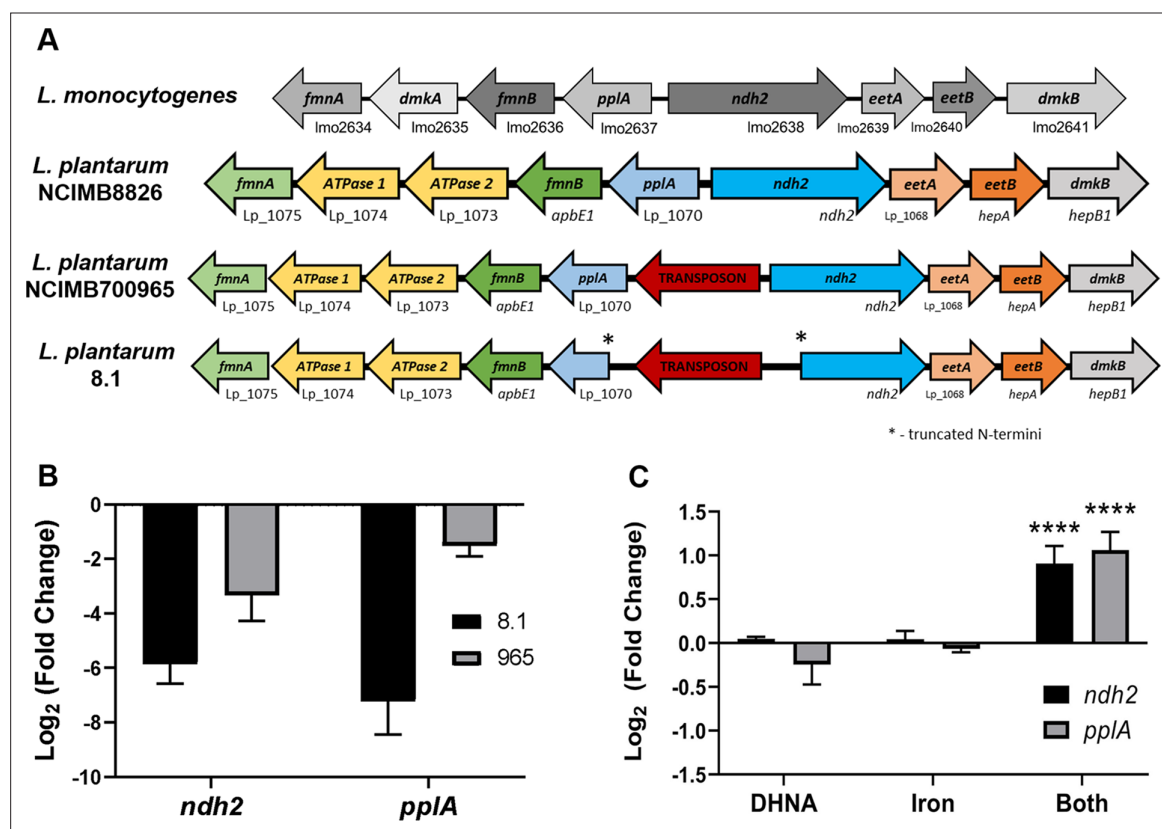


**Figure 2—figure supplement 2.** *ndh2* and *pplA* are required for iron reduction through EET. (A) Visualization of the FLEET locus in *L. monocytogenes* and three strains of *L. plantarum*. Genes are annotated based on predicted functions within the FLEET system. (B) Relative expression of *ndh2* and *pplA* in *L. plantarum* strains 8.1 and NCIMB700965 (“965”) during growth in MRS compared to *L. plantarum* NCIMB8826. The avg± stdev of three biological replicates is shown. (C) Relative expression of *ndh2* and *pplA* in *L. plantarum* during growth in mMRS containing 20 µg/mL DHNA, iron (1.25 ferric ammonium citrate), or both (DHNA and iron), compared to during growth in mMRS. Significant differences determined through Two-way ANOVA with Sidak’s post-hoc test (n = 3), \*\*\*\* p ≤ 0.0001. See related data in **Figure 2—figure supplement 2—source data 1**.

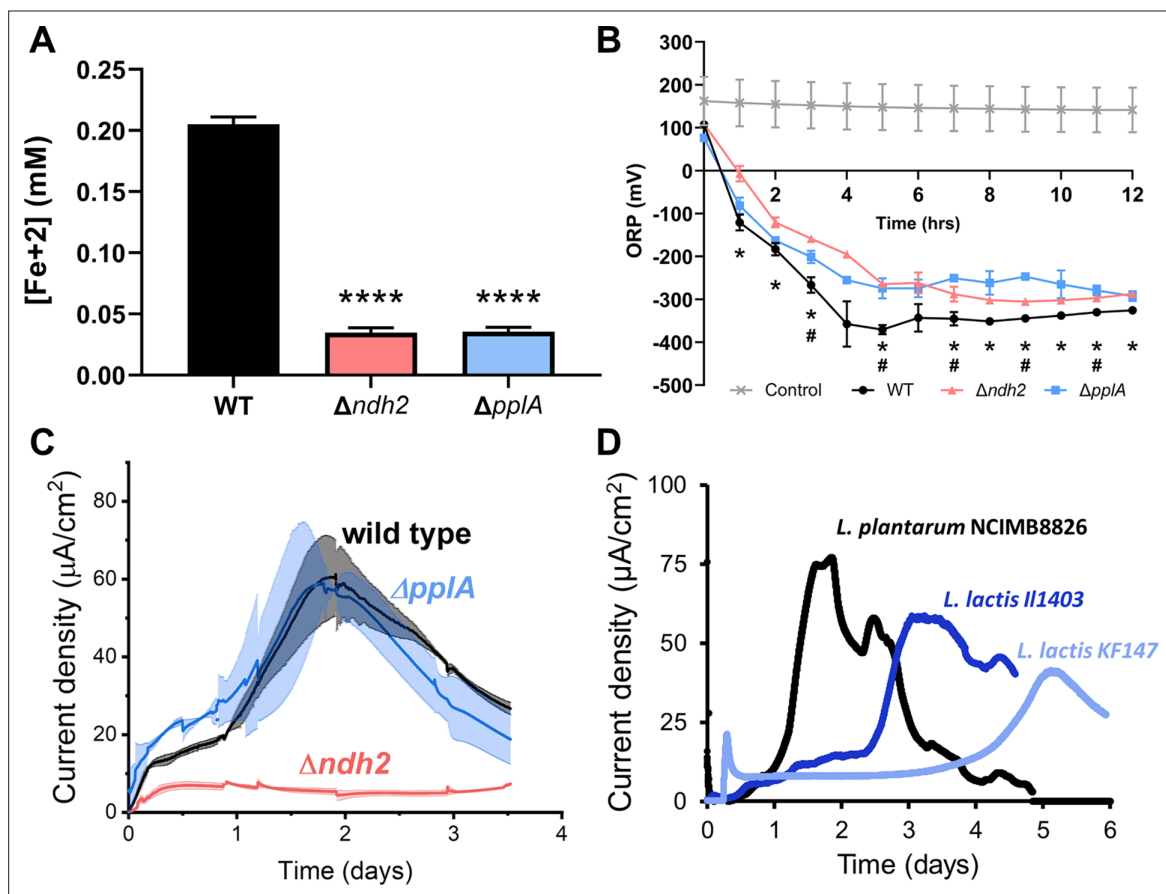


**Figure 3.** *L. plantarum* requires *ndh2* and conditionally *pplA* for EET. (A) Reduction of  $Fe^{3+}$  (ferrihydrite) to  $Fe^{2+}$  with wild-type *L. plantarum* or EET deletion mutants in the presence of 20  $\mu g/mL$  DHNA and 55 mM mannitol after growth in mMRS supplemented with 20  $\mu g/mL$  DHNA and 1.25 mM ferric ammonium citrate. Significant differences determined by one-way ANOVA with Dunnett's post-hoc test, \*\*\*\*  $p \leq 0.0001$ . (B) Redox potential of mMRS supplemented with 20  $\mu g/mL$  DHNA and 1.25 mM ferric ammonium citrate after inoculation with wild-type *L. plantarum* or EET deletion mutants. Significant ORP differences between the wild-type and mutant strains determined by two-way RM ANOVA with Tukey's post-hoc test, \*  $p < 0.05$  (WT vs.  $\Delta ndh2$ ); #  $p < 0.05$  (WT vs.  $\Delta pplA$ ). (C) Current density generated by wild-type *L. plantarum* and deletion mutants in mCDM supplemented with 20  $\mu g/mL$  DHNA. The avg  $\pm$  stdev is shown. (D) Current density generated by *L. plantarum* and two *L. lactis* strains lacking *pplA* in mCDM. For *L. plantarum*, the mCDM was supplemented with 20  $\mu g/mL$  DHNA. The data correspond to the average of two (D) or three (A to C) biological replicates per strain. See also **Figure 3—figure supplement 1** and **Figure 3—figure supplement 2** and related data in **Figure 3—source data 1**.

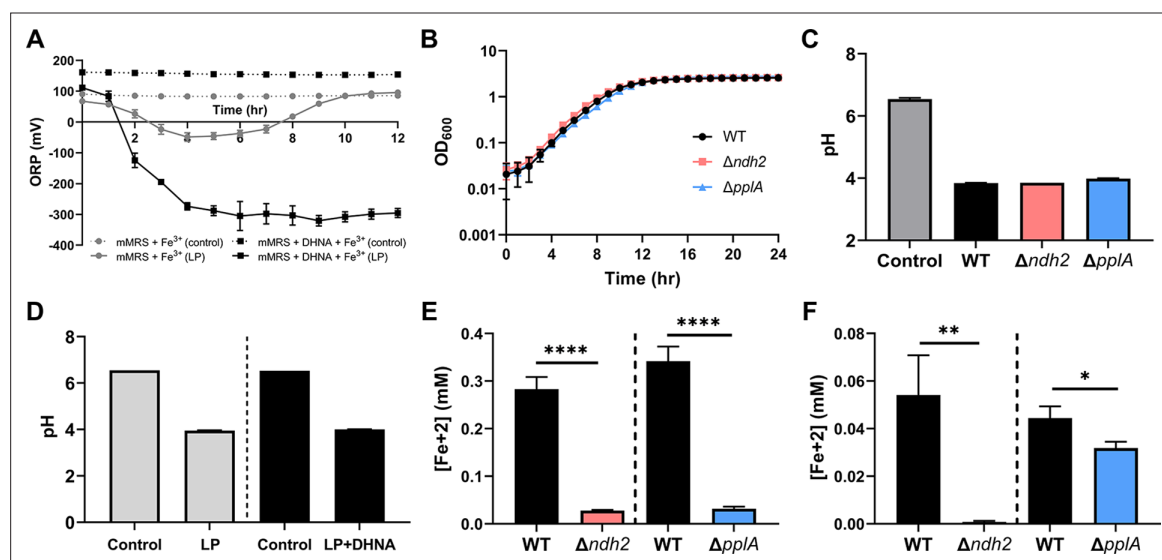


**Figure 3—figure supplement 1.** Impact of *ndh2* and *pplA* deletion on growth, iron reduction, current density, and metabolites production. **(A)** Redox potential of mMRS supplemented with 1.25 mM ferric ammonium citrate after inoculation with wild-type *L. plantarum*. Where indicated, 20  $\mu$ g/mL DHNA was supplemented as well. **(B)** Growth of wild-type *L. plantarum*,  $\Delta ndh2$ , or  $\Delta pplA$  in mMRS supplemented with 20  $\mu$ g/mL DHNA and 1.25 mM ferric ammonium citrate. **(C)** Final pH from **Figure 3B**. **(D)** Final pH from **Figure 3—figure supplement 1A**. **(E and F)** Reduction of ferrihydrite by *L. plantarum* or FLEET deletion mutants from **Figure 3B** in the ferrihydrite reduction assay at **(E)**  $\Delta V_{max}$  (~5 hr) or **(F)** stationary phase (12 hr). Significant differences determined through Two-tailed t-test ( $n = 3$ ), \*  $p \leq 0.05$ ; \*\*  $p \leq 0.01$ ; \*\*\*\*  $p \leq 0.0001$ . The avg  $\pm$  stdev of three biological replicates is shown. See related data in **Figure 3—figure supplement 1—source data 1**.

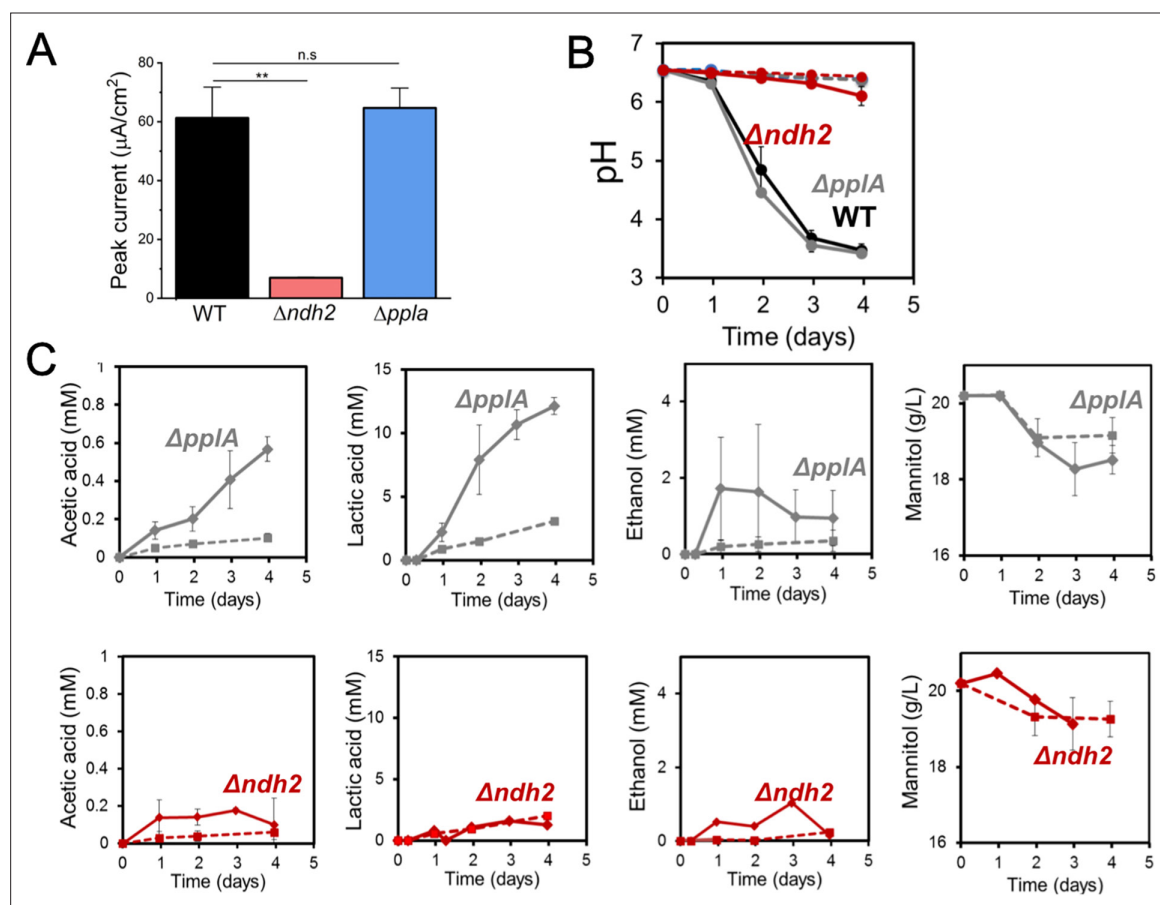


**Figure 3—figure supplement 2.** Impact of *ndh2* and *pplA* deletion on maximum current density, pH and metabolites production. **(A)** Peak current generated by wild-type *L. plantarum* or either the  $\Delta ndh2$  or  $\Delta pplA$  mutant from **Figure 3C**. **(B)** pH measurements and **(C)** metabolites produced in the bioelectrochemical reactors inoculated with wild-type *L. plantarum* or either the  $\Delta ndh2$  or  $\Delta pplA$  mutant from **Figure 3C**. Solid lines denote the presence of an anode polarized to +0.2 V (vs Ag/AgCl sat. KCl) while dashed lines denote open circuit conditions. See related data in **Figure 3—figure supplement 2—source data 1**.

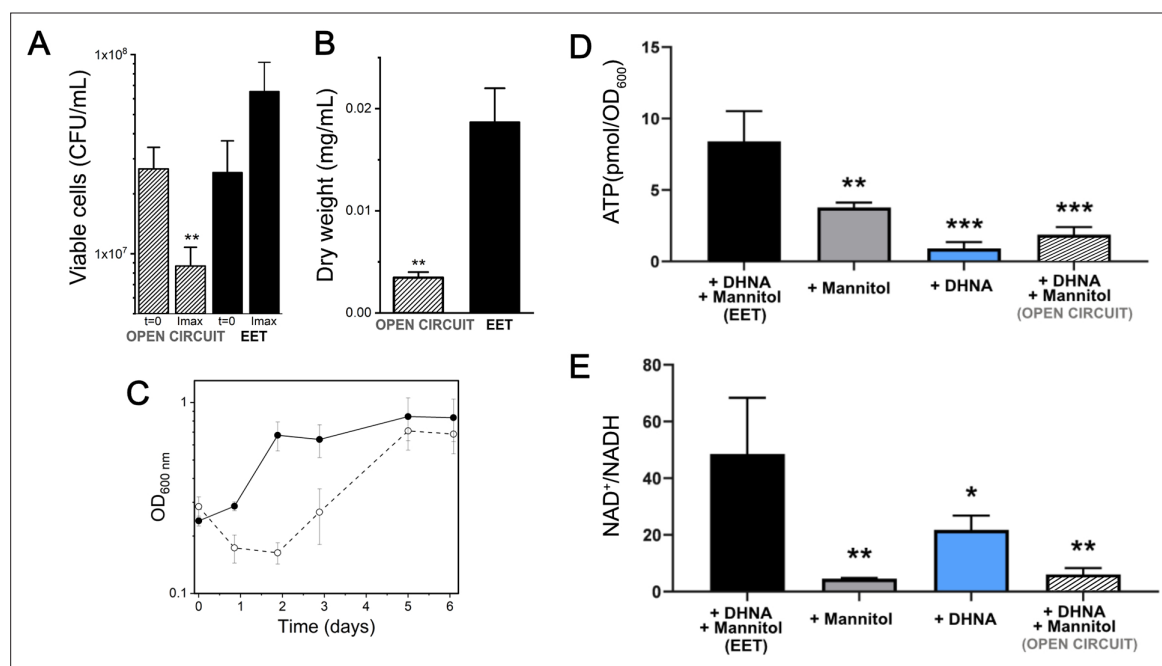


**Figure 4.** Growth, ATP, and redox balance of *L. plantarum* changes when an anode is provided as an extracellular electron acceptor. These measurements and the current density plot shown in **Figure 1C** are from the same experiment. **(A)** Viable cells and **(B)** dry weight at the point of maximum current density under current circulating conditions (EET) and at open circuit conditions (OC) at the same time point. **(C)** Change in cell numbers measured by OD<sub>600</sub> over time in the bioreactors under EET (continuous line) and OC conditions (dotted lines). **(D)** ATP production per OD<sub>600</sub> unit and **(E)** NAD<sup>+</sup>/NADH ratios at the point of maximum current density. The bioreactors were shaken vigorously to dislodge cells before sampling. The avg  $\pm$  stdev of three biological replicates is shown. Significant differences were determined by one-way ANOVA with **(A and B)** Dunn-Sidak post-hoc test ( $n = 3$ ), \*  $p < 0.05$ ; \*\*  $p < 0.01$ ; \*\*\*  $p < 0.001$ ; \*\*\*\*  $p < 0.0001$ . See also **Figure 1** panel C and **Figure 4—figure supplement 3** and related data in **Figure 4—source data 1**.



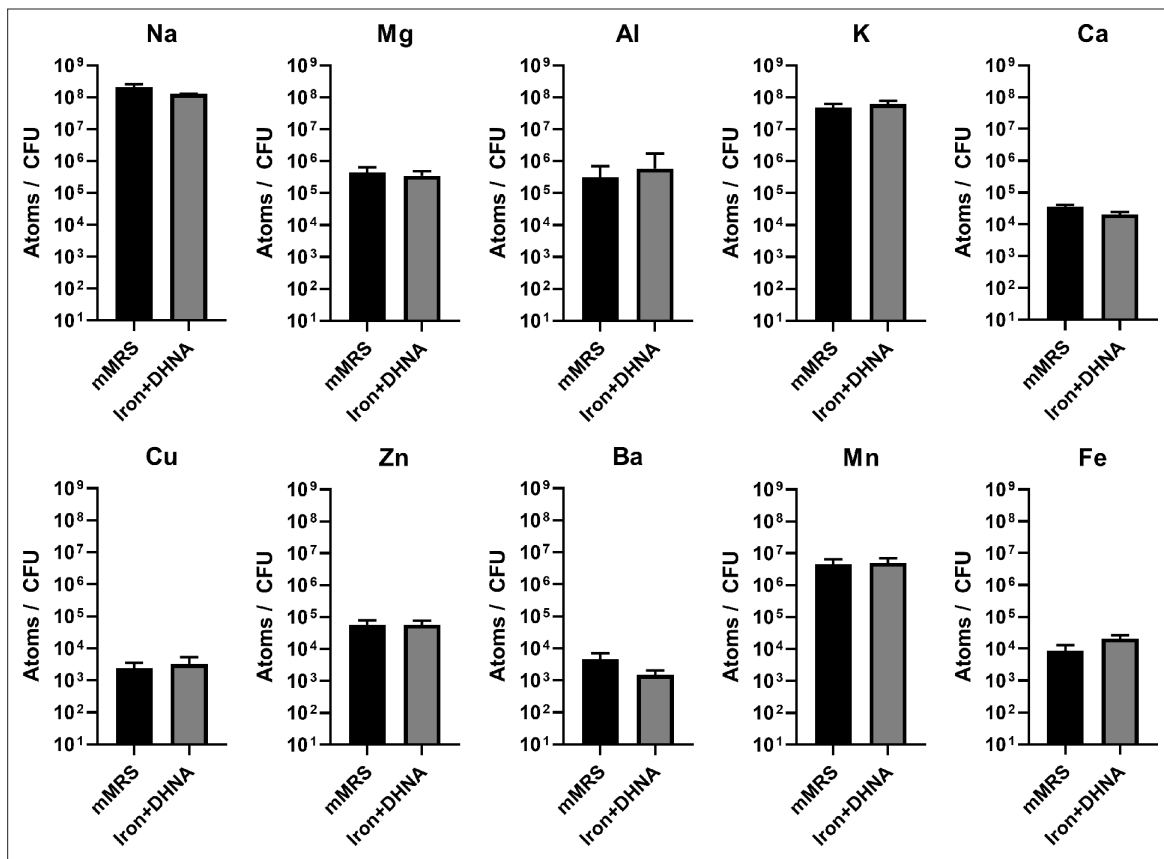


**Figure 4—figure supplement 1.** Intracellular metal concentrations in *L. plantarum* are not affected by EET-conductive growth conditions. Inductively coupled plasma mass spectrometry (ICP-MS) quantification of intracellular metals in *L. plantarum* after growth for 18 hr in mMRS or mMRS supplemented with 20 µg/mL DHNA and iron (1.25 mM ferric ammonium citrate). The avg± stdev of three biological replicates is shown. See related data in **Figure 4—figure supplement 1—source data 1**.

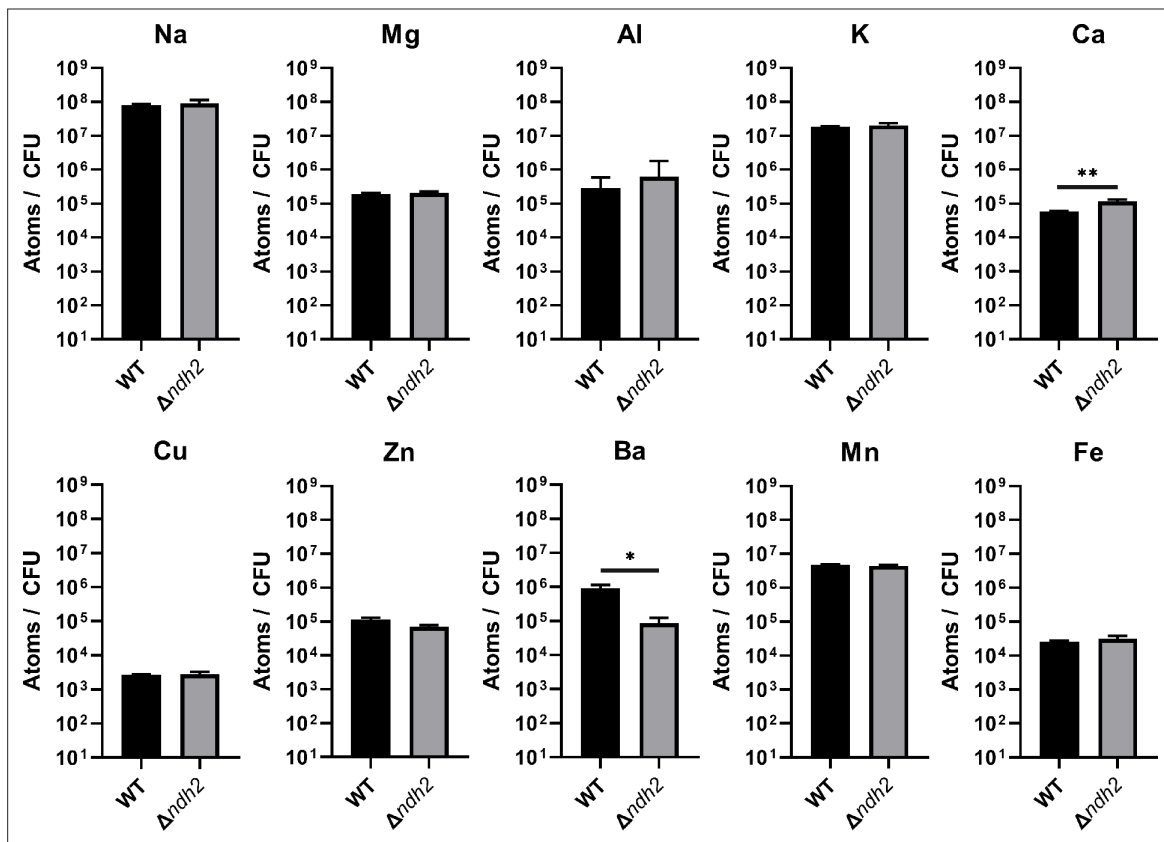


**Figure 4—figure supplement 2.** Redox-active metal concentrations in *L. plantarum* are not affected by the presence of *ndh2*. Inductively coupled plasma mass spectrometry (ICP-MS) quantification of intracellular metals in wild-type *L. plantarum* and a *L. plantarum ndh2* deletion mutant after growth for 18 hr in mMRS supplemented with 20  $\mu$ g/mL DHNA and iron (1.25 mM ferric ammonium citrate). The avg  $\pm$  stdev of three biological replicates is shown. Significant differences determined by one-way ANOVA with Dunnett's post-hoc test, \*  $p \leq 0.05$ ; \*\*  $p \leq 0.01$ . See related data in **Figure 4—figure supplement 2—source data 1**.

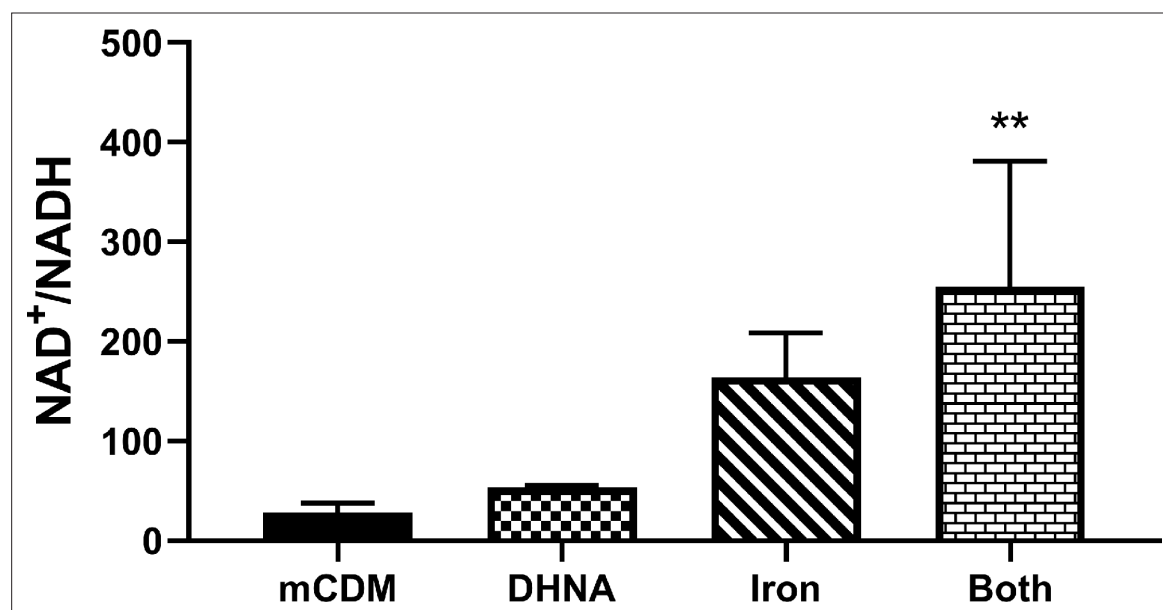


**Figure 4—figure supplement 3.** Use of Fe<sup>3+</sup> as an electron acceptor allows *L. plantarum* to regenerate NAD<sup>+</sup>. NAD<sup>+</sup>/NADH ratios of *L. plantarum* grown to mid-exponential phase in mCDM with/without the supplementation of 20 µg/mL DHNA, iron (1.25 mM ferric ammonium citrate), or both. The avg± stdev of three biological replicates is shown. Significant differences determined through one-way ANOVA with Dunnett's post-hoc test (n = 3), \*\* p ≤ 0.01. See related data in **Figure 4—figure supplement 3—source data 1**.

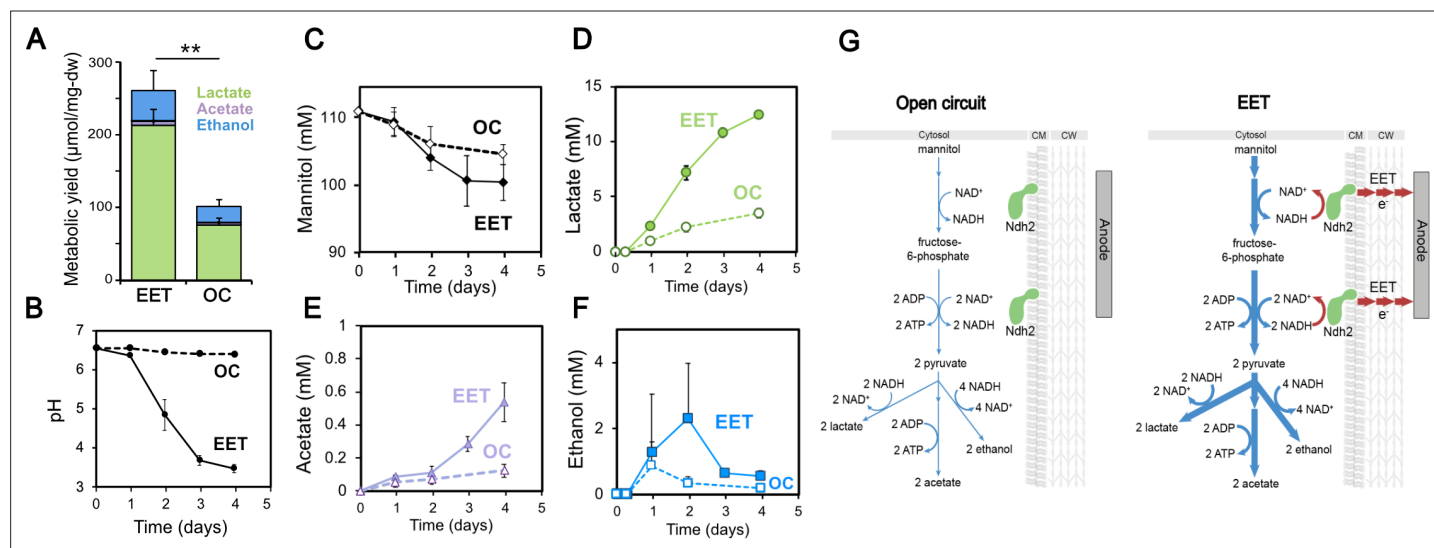


**Figure 5.** Fermentation fluxes are increased when an anode is provided as an extracellular electron acceptor. Results are from the same set of experiments as the current density plot shown in **Figure 3C**. **(A)** Metabolic yields of *L. plantarum* end-fermentation products under open circuit conditions (OC) and current circulating conditions (EET) in mCDM supplemented with 20 μg/mL DHNA. **(B)** pH measurements and **(C)** mannitol, **(D)** lactate, **(E)** acetate, and **(F)** ethanol concentrations over time under OC and EET conditions. **(G)** Schematic of proposed model for NADH regeneration during fermentation of mannitol in the presence of an anode as electron sink for *L. plantarum*. The avg ± stdev of three biological replicates is shown. Significant differences were determined by one-way ANOVA with Dunn-Sidak post-hoc (n = 3), \*\* p ≤ 0.01. See also **Figure 5—figure supplement 1** and **Figure 5—figure supplement 2** and related data in **Figure 5—source data 1**.

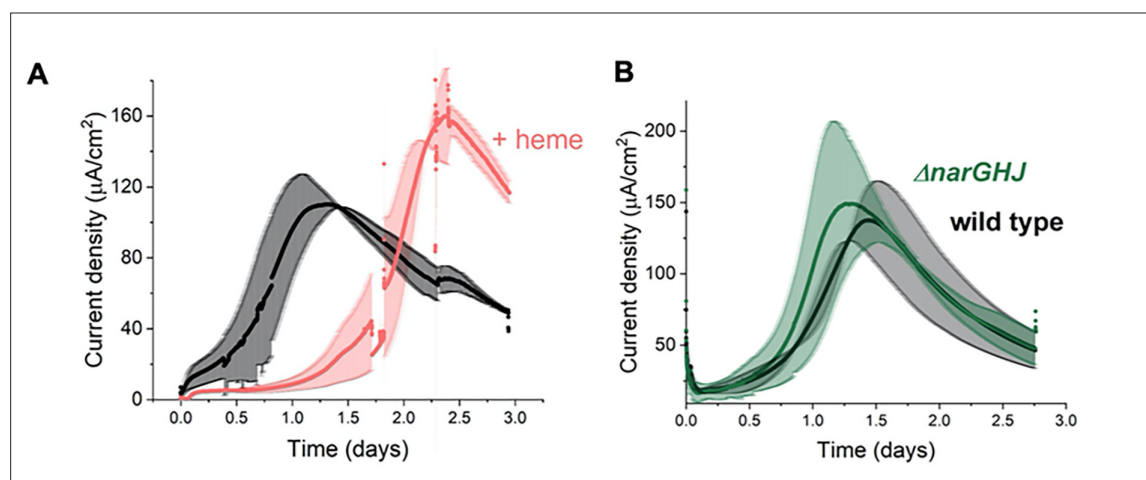


**Figure 5—figure supplement 1.** EET by *L. plantarum* is not dependent on aerobic or anaerobic respiration components. **(A)** Effect on *L. plantarum* current production with heme addition to reconstitute the aerobic electron transport chain. **(B)** Effect on *L. plantarum* current production with the deletion of the nitrate reductase A. The anode was polarized to +0.2 V (vs Ag/AgCl sat. KCl). The avg $\pm$  stdev of two biological replicates is shown. See related data in **Figure 5—figure supplement 1—source data 1**.

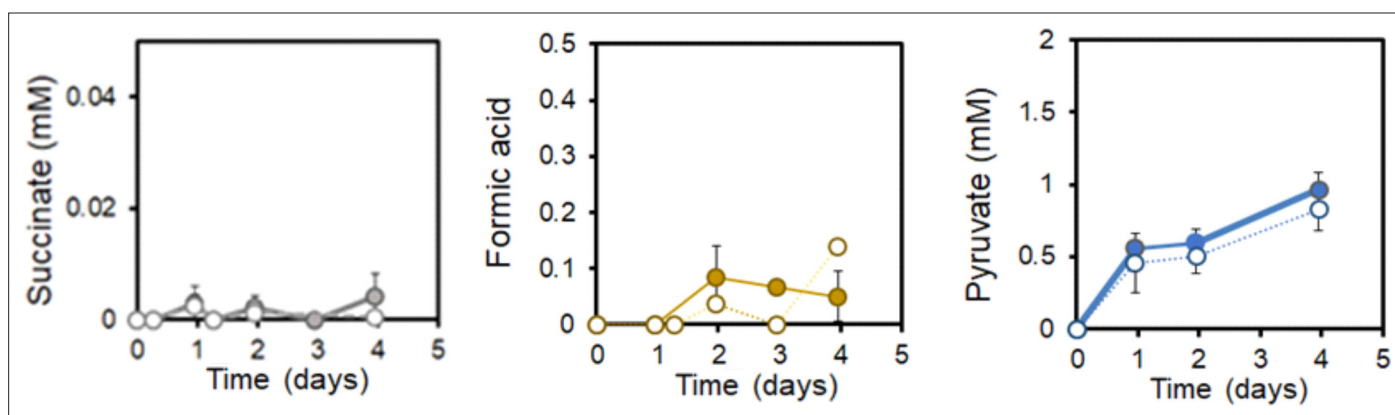


**Figure 5—figure supplement 2.** EET by *L. plantarum* does not involve TCA cycle metabolites. Succinate, formate and pyruvate produced under EET (solid line) and open-circuit (dashed line) conditions from **Figure 5**. The avg± stdev of three biological replicates is shown. See related data in **Figure 5—figure supplement 2—source data 1**.

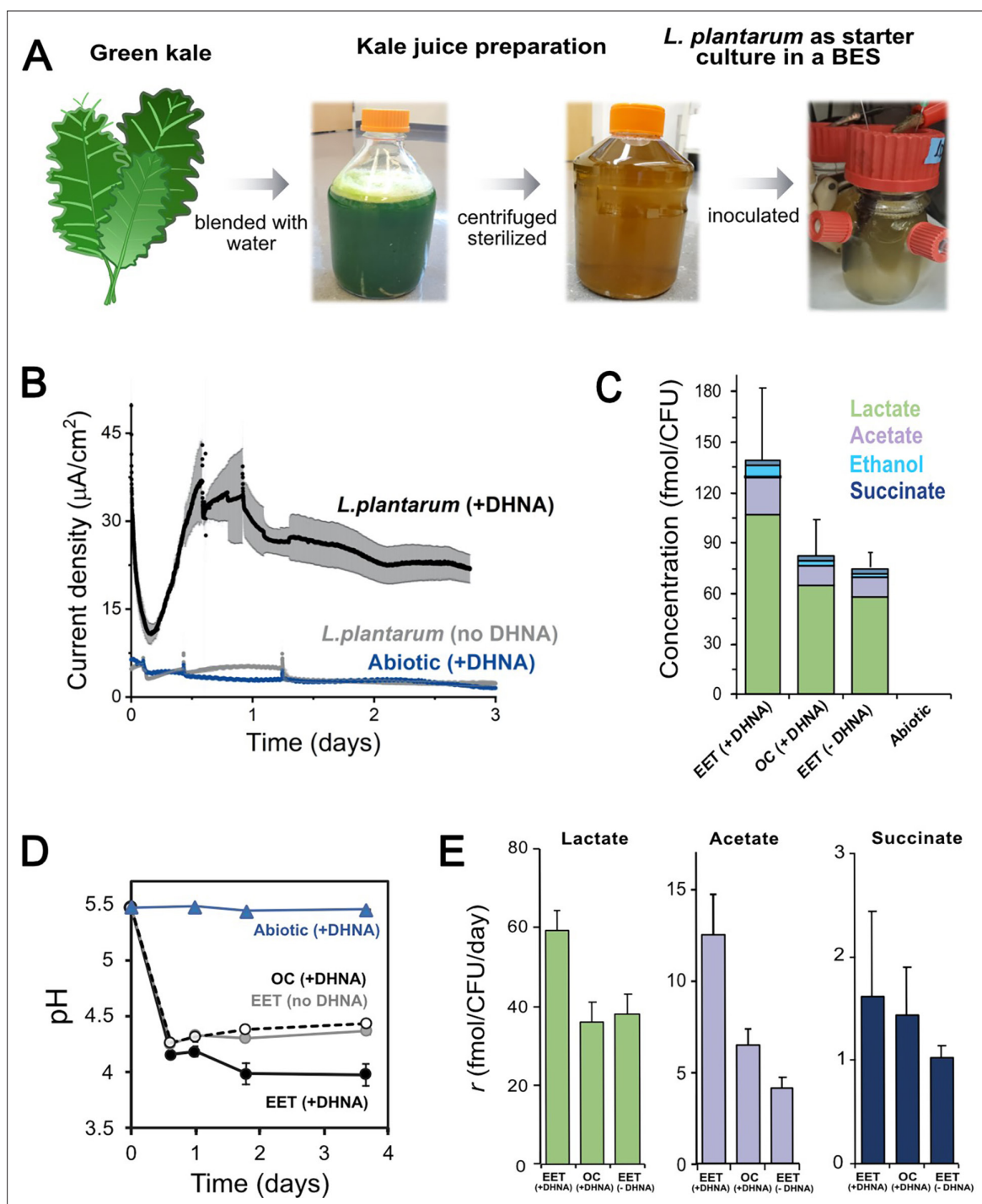


**Figure 6.** EET in a kale juice increases the production of fermentation end products. **(A)** Preparation of kale juice medium used for fermentation in bioelectrochemical reactors. **(B)** Current density production measured from kale juice medium over time in the presence of *L. plantarum* and 20  $\mu\text{g}/\text{mL}$  DHNA, no DHNA, or under abiotic conditions with addition of 20  $\mu\text{g}/\text{mL}$  DHNA. The anode polarization was maintained at 0.2  $V_{\text{Ag}/\text{AgCl}}$ . **(C)** Normalized total quantities of the metabolites detected per cell ( $\text{CFU}_{\text{max}}$  used for calculations). **(D)** pH measurements over time under different conditions tested on a second set of kale juice fermentations performed under the same conditions. **(E)** Production rate per viable cell,  $r$ , of lactate, acetate, and succinate. The avg  $\pm$  stdev of three biological replicates is shown. See also **Figure 6—figure supplement 1** and related data in **Figure 6—source data 1**.

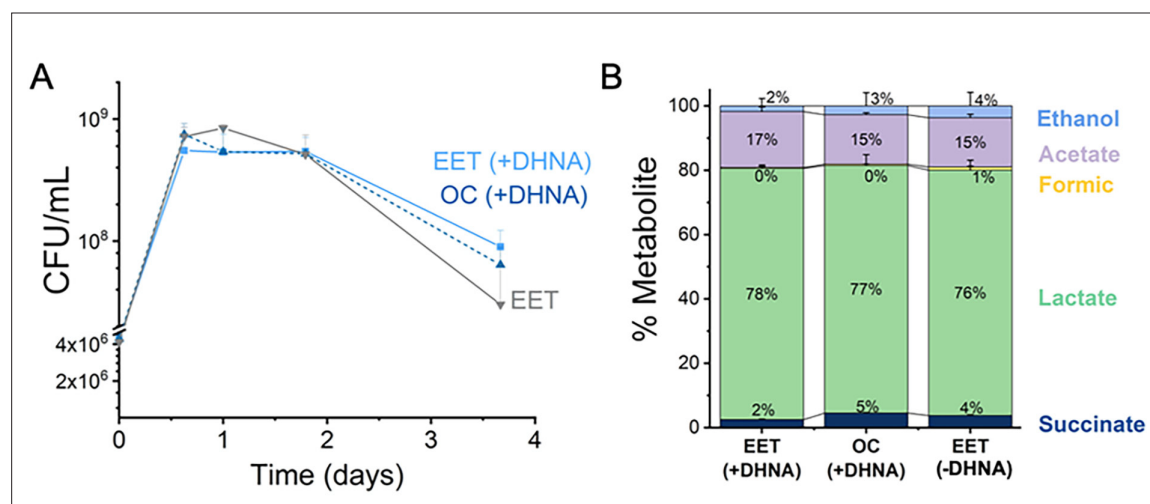


**Figure 6—figure supplement 1.** EET does not impact cell viability and distribution of metabolites in a kale fermentation. **(A)** Viable cells of *L. plantarum* NCIMB8826-R during the fermentation of kale juice in the presence of a polarized anode with/without DHNA, and under open circuit conditions with DHNA. **(B)** Distribution of metabolites after 2 days of kale juice fermentation. The anode polarization was maintained at +0.2 V (vs Ag/AgCl sat. KCl). The avg± stdev of three biological replicates is shown. See related data in **Figure 6—figure supplement 1—source data 1**.